AEROGASDYNAMICS OF WAVERIDERS WITH POWER-LAW COMPRESSION SURFACES

I.I. Mazhul and R.D. Rakhimov

Institute of Theoretical and Applied Mechanics SB RAS,
630090 Novosibirsk, Russia

Use of the well-known flows streamlines with specified properties to design spatial lifting configurations (waveriders) allows to simplify essentially an analysis of such form characteristics in the so-called design flow regimes which corresponds to their construction conditions. Waveriders using as the basis of a future hypersonic aircraft is widely discussed. Waveriders characteristics in the design regimes have been analyzed in a number of works. However, the off-design regimes applying to a hypersonic aircraft should be investigated. The investigations of such types are more limited, and for some classes of the waveriders they are absent at all.

Hereinafter, the investigations results of the waveriders designed using the flows behind planar shock waves as basic flows are presented. A body surface is described by a power-law functions that allow to obtain a series of configurations with different cross-section shapes, including, as a particular case, a widely known Nonweiler caret wing. Estimations of lift-to-drag ratio and integral heat fluxes to the surface in the design regimes are presented, and in the frames of the Euler equations the flow in the off-design regimes is numerically studied. It were considered flow patterns at both smaller and larger free-stream flow Mach numbers M_∞ of some design M_d, at which the configuration was constructed.

Waveriders surface

It is considered the waveriders derived on the basis of the flow behind planar shocks for whose surface analytical description the power-law functions are used. Then, a form of the leading edges in a plan view, of the lower and upper surfaces contours in any cross-section x may be set as follows:

$$z_{pl} = A\, x^n \quad ,$$

$$y_l = -x\, tg\delta - (tg\beta - tg\delta)\,(z/A)^{1/n} \quad ,$$

$$y_u = -tg\beta\,(z/A)^{1/n}$$

accordingly. Here A is a constant coefficient, n is an exponent, β is an oblique shock inclination angle, δ is a flow deflection angle behind the shock in the basic flow (a wedge compression angle), x,y,z is the Cartesian coordinate system which begins in the body nose. Here $0 < x \le L$, $0 \le z \le z_{pl}$, $0 < n < \infty$, and $0 < A < \infty$, L is the body length. General view of configuration and nomenclature are presented in Fig. 1.

To describe the waveriders surfaces of such type five independent parameters should be set: A, n, δ, β (or the design Mach number M_d), L. Let us mark two special points by change of the exponent n. Thus, at $n = 1$ we have the waveriders with linear leading edges and linear spanwise surface contours, i.e. the known Nonweiler`s caret wing. With decreasing of n the leading edges and spanwise contour become less convex, and in the limit at $n \Rightarrow 0$, we obtain the linear non-swept leading edge and the waverider in the form of wedge with side cheeks. In the region of $n > 1$ a convex form of the leading edge as well as the spanwise contour is observed, and by large values of n "narrow" configurations are realized, which are not of

Report Documentation Page

Report Date	Report Type	Dates Covered (from... to)
23 Aug 2002	N/A	-

Title and Subtitle Aerogasdynamics of Waveriders With Powder-Law Compression Surfaces	**Contract Number**
	Grant Number
	Program Element Number
Author(s)	**Project Number**
	Task Number
	Work Unit Number
Performing Organization Name(s) and Address(es) Institute of Theoretical and Applied Mechanics Institutskaya 4/1 Novosibirsk 530090 Russia	**Performing Organization Report Number**
Sponsoring/Monitoring Agency Name(s) and Address(es) EOARD PSC 802 Box 14 FPO 09499-0014	**Sponsor/Monitor's Acronym(s)**
	Sponsor/Monitor's Report Number(s)

Distribution/Availability Statement
Approved for public release, distribution unlimited

Supplementary Notes
See also ADM001433, Conference held International Conference on Methods of Aerophysical Research (11th) Held in Novosibirsk, Russia on 1-7 Jul 2002

Abstract

Subject Terms

Report Classification unclassified	**Classification of this page** unclassified
Classification of Abstract unclassified	**Limitation of Abstract** UU

Number of Pages
6

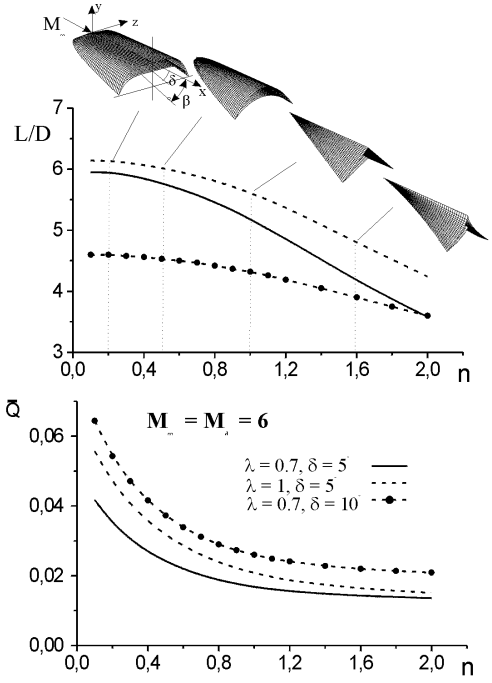

Fig.1

practical interest. To describe the surface it is also necessary to set the coefficient A, which may change in the limits of $0 < A < \infty$, as it was earlier noted. Its value may be chosen on a basis of integral geometrical characteristics specification (volume, planform area, aspect ratio and etc.) or of the local characteristics of the leading edge and spanwise contour (sweep angle of the leading edge, inclination angles of spanwise contour in any cross-section $x = \text{const}$). Further, the coefficient values A are determined according to the aspect ratio of configuration in the form of $A = \lambda/[2(n+1)L^{n-1}]$, where $\lambda = l^2/S_{pl}$ is aspect ratio, l is span, S_{pl} is the planform area.

Method of calculation

To analyze the waveriders characteristics in the design regimes the analytical solutions for the flow behind the oblique shocks and integral methods of turbulent boundary layer calculation were used. Data correspond to a free stream dynamic pressure $q_\infty = 7\ 10^4$ N/m^2. Integral heat flux to the surface Q was obtained as a difference between the convective heat flux to a body and radiation flux from a body for a prescribed surface temperature $T_w = 800$ K. Further, it is normalized to a free-stream heat content ΔQ_0 per unit area that characterizes a heat quantity which can be obtained from the free-stream by its adiabatic compression up to $M_\infty = 0$ and T_0.

An algorithm of Euler equations numerical solution described in detail in [1, 2] was used to study three-dimensional inviscid supersonic steady-state flow on the off-design regimes near the considered waveriders configurations. Integration along a marching direction was performed by using TVD-schemes of the high approximation order (up to third) which conserve the solution monotonicity. This allows to capture gasdynamic discontinuities without introducing of artificial viscosity. The fluxes on the sides between the computational cells have been determined from the solution of a supersonic flows interaction problem using the Harten-Lax-van Leer-Einfeldt method. To reconstruct the parameters on the cells sides from their volume-averaged values the MUSCL van Leer method of the third order approximation was applied.

Calculation results

The main parameter which determines the planform and spanwise contour as well as aerodynamic characteristics of waveriders of the considered types is power-law exponent n. Lift-to-drag ratio L/D and integral heat fluxes to the surface $\bar{Q} = Q/\Delta Q_0$ in the design regimes as well as the waveriders shapes changing by variations of n are presented in Fig.1. With decreasing of n lift-to-drag ratio and integral heat fluxes decrease independently on the values of λ and δ. In particular, the values of L/D are higher than for the caret wing. By this, the

spanwise contour of the lower surface becomes less convex, and it is appeared a constructive possibility to mount on a flat scramjet inlet. More detailed analysis of aerodynamic characteristics in the design regimes may be found in [3].

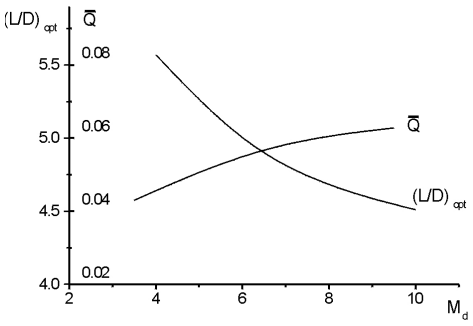

Fig. 2.

Choice of waveriders optimal configurations satisfied to numerous demands shall depend on flying conditions and purpose of aircraft. Usually, lift-to-drag ratio is considered as optimization criteria. However, to provide large volumes and low levels of integral heat fluxes Q to the surface can be also essential for hypersonic aircraft. Therefore, it is advisable to consider all three mentioned conditions. For these purposes the design variables were optimized for the objective function given by $F(n,\delta,\lambda) = (L/D)V^{2/3}/S_w$, where V is a volume, S_w is a body wetted area that determines the possible level of Q at a considerable degree. The example of such optimization is shown in Fig. 2, which presents a lift-to-drag ratio and values of integral heat fluxes. In particular, in the range of M_d = 4-10 values δ_{opt} = 8.2-9.1°, n_{opt} = 0.37-0.32, i.e. they are changed insignificantly. But aspect ratio λ is decreased from 1.07 to 0.55 with increasing Mach number M_d = 4 to M_d = 10.

Change of the flow structure by possible variations of n in the regimes $M_\infty > M_d$ is shown in Fig. 3, which presents relative density ρ/ρ_∞ contours in the base sections $x = L$ for the configuration with $M_d = 6$, $\delta = 5°$, $\lambda = 0.7$ at $M_\infty = 8$ and the angle of attack $\alpha = 0$. For configuration with $n \sim 1$ a Mach interaction of the shocks is observed. In the flow structure some shocks may be separated: a central shock due to a flow turn in a plane of symmetry; a shock attached to the leading edges; and, resulting from their interaction an inner shock falling on the body surface. A slip line, beginning from a triple point of the shocks cross and directed to an angle point in the plane of symmetry is observed. However, at values of $n < 0.8$ a degeneration of the inner shock is found, and it is occurred an isentropic flow compression.

Some flow details may be defined more precisely according to the distribution data of the relative pressure p/p_∞ along the lower surface in the considered section $x = L$ that is presented in Fig. 4, where $z' = 2z/l$, l is a section span.

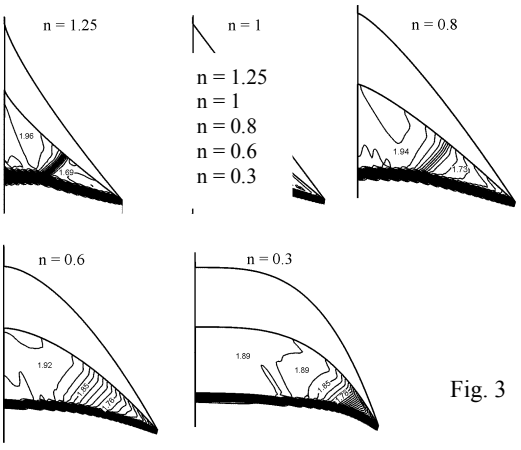

Fig. 3

In particular, let us note a different flow character in region between the leading edges and the inner shock front by the configuration variation relatively to $n \sim 1$. Thus, for n = 1.25 the flow expansion and the pressure decrease directed to the body symmetry plane are observed; for n = 0.8 is quite contrary, the flow compression is seen. It was due to the corresponding curvature sign change of the lower surface spanwise contour at crossing the point n = 1. Here, a higher pressure level both for own leading edges and in the symmetry plane region for the case when n = 1.25 is

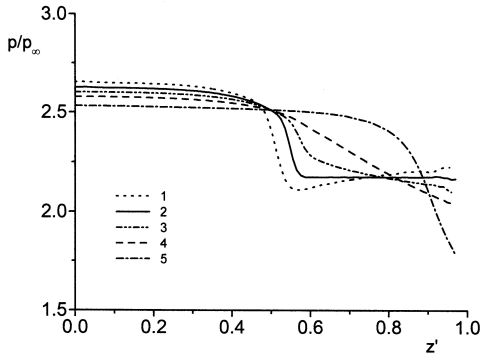

Fig. 4.

observed. It follows from presented pressure distributions that the inner shock intensity in the last case is also higher and is decreased with decreasing of the parameter n.

As it was mentioned above, with decreasing of n the inner shock is moved in the direction of leading edges and then is degenerated. For the considered values $n \le 0.6$ the flow behind the attached on the leading edges shock has isentropic character with a smooth pressure increase to the plane of symmetry. In case for configurations with the exponents $n \le 0.3$ in a large body span $0 \le z' < 0.7$ an uniform distribution of the pressure and an uniform flow field between the surface and shock are observed. Thus, for $n = 0.3$ the Mach number and the body pressure non-uniformity in the noted region are 3.4% and 2.2% accordingly, and between the body surface and the shock wave in the symmetry plane is about 0.02% and 0.2%. In combination with the sufficiently smooth spanwise contour of the lower surface in the noted region it is also a favorable factor by considering it as a surface of pre-compression for scramjet inlet of perspective hypersonic vehicles.

Flow near the considered configurations is not conical excluding the variant with $n = 1$. Figure 5 shows the pressure distribution along the lower surface span and the density contours in several cross-sections x = const for the waveriders with $n = 1.25$ at $M_\infty = 8$ and the angle of attack $\alpha = 0$ ($M_d = 6$, $\delta = 5°$, $\lambda = 0.7$). With transition along a configuration length to the base section intensity of the shock in the leading edge is increased, that is probably due to increasing of the normal to the leading edge velocity component because of wing sweep decreasing. The other way, the inner shock intensity is decreased. At this, the inner shock with decreasing of the relative coordinate $x' = x/L$ is moved in direction of the symmetry plane. For all values of x' in the region between the leading edge and inner shock on the body surface the pressure decrease is observed, i. e a flow expansion is taken place. The noted flow properties are also seen in the density distribution contours in the spanwise sections and on the lower body surface in the plane of xz.

The other regularities are seen for the waveriders with the parameter of $n < 1$. For example, at $n = 0.8$ (Fig. 6a) the shock intensity on the leading edge is decreased along a body length. The inner shock intensity is increased, and it moves to the leading edge. In the region between the leading edge and inner shock the pressure is slightly increased, i.e. isentropic flow compression is realized. For configurations with $n = 0.3$ (Fig. 6b) the inner shock is lacking, an isentropic compression is observed behind the shock attached to the leading

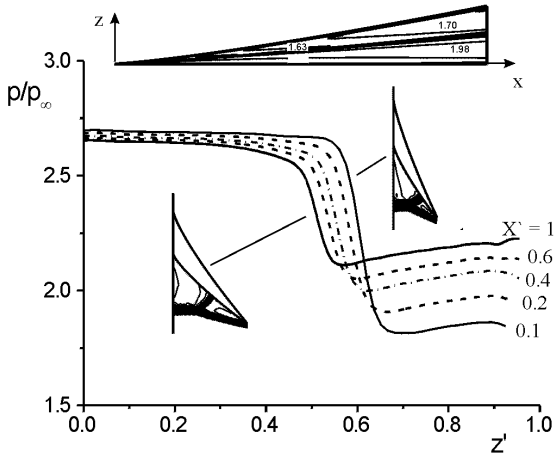

Fig. 5.

edge whose intensity is increased with increasing of x'. At this, the pressure distribution in the region of $0 \le z' < 0.7$ is uniform enough practically on the whole lower surface.

The example of the waverider configuration with $n = 0.3$ was used to consider a change of a flow structure near the lower surface by increase of the angles of attack. As it was noted above, at small values of $\alpha \sim 0$ in the leading edge region the isentropic compression flow is observed. However, even at $\alpha \sim 3°$ in the cross-sections $x \sim L$ near the leading edge a formation of the inner shock and a shock wave Mach configuration is observed as a whole, although isentropic compression region near the leading edge is also kept. The data of Fig. 7c show that the inner shock intensity is increased versus the angle of attack. At large α immediately behind the inner shock front a flow expansion region and a sufficien-tly sharp pressure decreasing are seen that is due to necessity of an additional flow deflection behind the inner shock to the symmetry plane. Nevertheless, in the region $z' < 0.7$-0.8 the flow near the lower surface remains the uniform enough in all angles of attack range under studied.

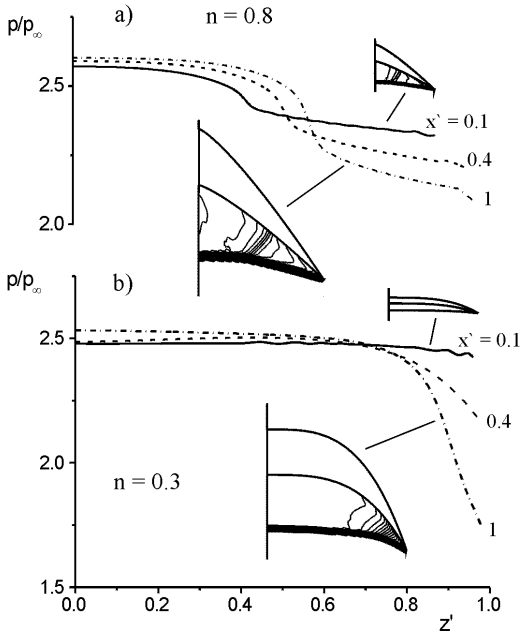

Fig. 6.

With increasing of α the inner shock begins to form closer to a body nose. Flow pattern in the form of a density distribution on the lower surface in the plane xz and in the cross-section $x' = 1$ by the angle of attack $\alpha = 9°$ is shown in Fig. 7a (the levels ρ/ρ_∞ are noted) and 7b accordingly.

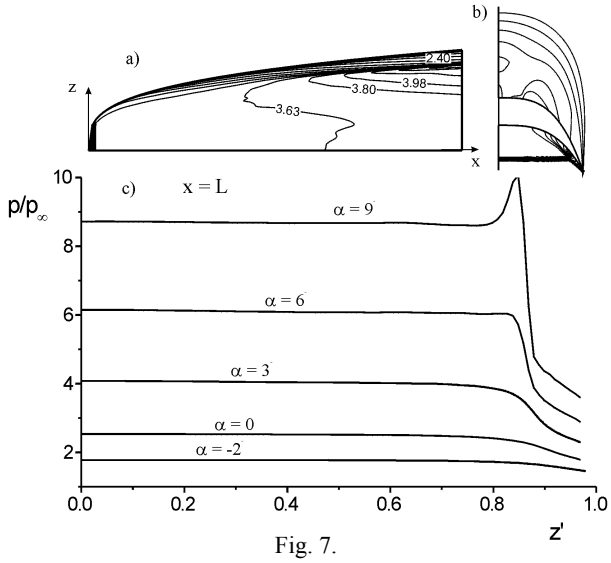

Fig. 7.

Flow patterns of the considered configurations ($M_d = 6$, $\delta = 5°$, $\lambda = 0.7$) at the free-stream Mach $M_\infty = 4$, i.e. in regimes at $M_\infty < M_d$ was also studied. As the calculations show, for the waveriders with the parameter $n \ge 1$ a flow with detached shock on the leading edges along the whole body is observed. However, in case of the configuration with exponent $n < 1$ it may be observed a flow peculiarity connected with different flow regimes on the

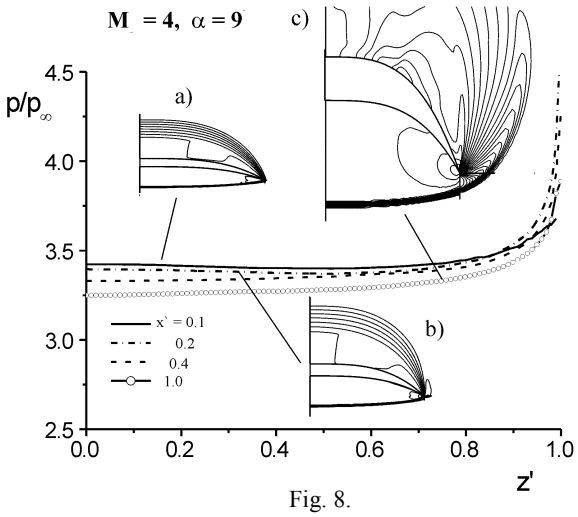

Fig. 8.

leading edge: with the attached shock at small values of x' and with detached shock at higher x' . With increasing of the angle of attack a shock detachment point is moved somewhat forward along the leading edge.

As an example Figure 8 presents the pressure distribution along the surface and the density contours in different cross-sections for the configurations with $n = 0.3$ at the angle of attack $\alpha = 9°$. In the section $x' = 0.1$ the shock is attached to the leading edge, at $x' = 0.2$ onset of shock detaching and disturbance propagation into the upper surface region is observed. In the investigated range of $\alpha = –2\text{-}9°$ the pressure distribution on the body surface in all cross-sections is uniform in the region $0 \le z' < 0.8$.

Conclusion

The inviscid flow pattern of waveriders designed on the basis of planar flow behind the oblique shock was investigated. To describe such waveriders the power-law functions were used. In the regimes corresponding to the free-stream Mach numbers $M_\infty > M_d$ the inner shock degeneration and flow transition with Mach shocks interaction to a flow with one concave shock and isentropic compression in the leading edge region in case of the exponent decreasing up to the value of $n \sim 0.6$ and less is shown. Different flow character in the leading edge region and different character of the inner shock dislocation (when it is available) for the configurations with $n > 1$ and $n < 1$ in the given regimes are revealed. It was shown that for the configurations with the parameter $n < 0.5$ the flow field in the region of $0 \le z' \le 0.7\text{-}0.8$ remains uniform both in the regimes $M_\infty < M_d$ and $M_\infty > M_d$, that is a favorable factor to use such configurations as the basis of perspective hypersonic aircraft.

REFERNCES

1. **Kudryavtsev A.N., Rakhimov R.D.** A marching procedure of numerical solution of two-dimensional and three-dimensional steady Euler equations using shock-capturing schemes // Intern. Conf. on the Methods of Aerophysical Research: Proc. Pt 1. Novosibirsk, 1998. P.117–122.
2. **Goonko Yu.P., Kharitonov A.M., Kudryavtsev A.N., Mazhul I.I., Rakhimov R.D.** Euler simulations of the flow over a hypersonic convergent inlet integrated with a forebody compression surface // European Congress on Computational Methods in Applied Science and Engineering, Barcelona, 11-14 September 2000. CD-Rom Proceedings.
3. **Mazhul I.I.** Waveriders with power-law cross-section shapes // Thermophysics and Aeromechanics. 2002. No.1.